

1 Assessing Net Community Production in a Glaciated Alaska Fjord

2 Stacey C. Reisdorph^{1*} and Jeremy T. Mathis^{1,2}

3

4 ¹University of Alaska Fairbanks

5 Ocean Acidification Research Center

6 245 O'Neill Bldg.

7 P.O. Box 757220

8 Fairbanks, AK 99775-7220

9 907-474-5995

10

11 ²NOAA - Pacific Marine Environmental Laboratory

12 7600 Sandpoint Way NE

13 Seattle, WA 98115

14

15 *Correspondence to: S.C. Reisdorph (screisdorph@alaska.edu)

16

17 **Abstract**

18 The impact of deglaciation in Glacier Bay has been observed to seasonally influence the

19 biogeochemistry of this marine system. The influence from surrounding glaciers,

20 particularly tidewater glaciers, has the potential to effect the efficiency and structure of

21 the marine food web within Glacier Bay. To assess the magnitude, spatial and temporal

22 variability of net community production in a glaciated fjord, we measured dissolved

23 inorganic carbon, inorganic macronutrients, dissolved oxygen and particulate organic

1 carbon between July 2011 and July 2012 in Glacier Bay, AK. High net community
2 production rates were observed across the bay (~ 54 to ~ 81 mmol C m⁻² d⁻¹) between the
3 summer and fall of 2011. However, between the fall and winter, as well as between the
4 winter and spring of 2012, air-sea fluxes of carbon dioxide and organic matter respiration
5 made net community production rates negative across most of the bay as inorganic
6 carbon and macronutrient concentrations returned to pre-bloom levels. The highest
7 organic carbon production occurred within the west arm between the summer and fall of
8 2011 with $\sim 4.5 \times 10^5$ kg C d⁻¹. Bay-wide, there was carbon production of $\sim 9.2 \times 10^5$ g C d⁻¹
9 between the summer and fall. Respiration and air-sea gas exchange were the dominant
10 drivers of carbon chemistry between the fall and winter of 2012. The substantial spatial
11 and temporal variability in our net community production estimates may reflect glacial
12 influences within the bay, as melt-water is depleted in macronutrients relative to marine
13 waters entering from the Gulf of Alaska in the middle and lower parts of the bay. Further
14 glacial retreat will likely lead to additional modifications in the carbon biogeochemistry
15 of Glacier Bay with unknown consequences for the local marine food web, which
16 includes many species of marine mammals.
17

1 **1.0 Introduction**

2 Glacier Bay lies within the Gulf of Alaska (Gulf of Alaska) coastal ocean and is a
3 pristine glacially influenced fjord that is representative of many other estuarine systems
4 that border the Gulf of Alaska (Fig. 1). Glacier Bay is influenced by freshwater input,
5 primarily from many surrounding alpine and tidewater glaciers. The low-nutrient influx
6 of freshwater into Glacier Bay, which is highest (up to ~40% freshwater in surface waters
7 during the summer; Reisdorph and Mathis, 2014) along the northern regions of the bay,
8 affects the nutrient loading and, thus, biological production and carbon dioxide (CO₂)
9 fluxes within the bay. The southern region of the bay is less affected by this runoff due to
10 distance from the glacial influence and is more influenced by marine waters that
11 exchange through a narrow channel with a shallow entrance sill (~25 m).

12 Over the past ~250 years, Glacier Bay has experienced very rapid deglaciation,
13 which has likely impacted the biological structure of the bay. As the climate continues to
14 warm, additional changes to this ecosystem and marine population have the potential to
15 impact net community production (NCP) within the bay, with cascading effects through
16 the food web. To better understand the seasonal dynamics of the underlying
17 biogeochemistry in Glacier Bay, we used the seasonal drawdown of the inorganic
18 constituents of photosynthesis within the mixed layer to estimate regional mass flux of
19 carbon and rates of NCP along with air-sea flux rates of CO₂. This approach has been
20 used in other high-latitude regions to assess ecosystem functionality (e.g. Mathis et al.,
21 2009; Cross et al, 2012; Mathis and Questel, 2013), including net community production
22 and carbon cycling.

23 Previous studies have shown there is wide-ranging variability in rates of primary

1 production within other glaciated fjord systems, though NCP data within these
2 ecosystems are sparse. Fjords within the Central Patagonia region (48°S – 51°S) are
3 strongly influenced by glaciated terrain and freshwater runoff, similar to influences in
4 and around Glacier Bay. A study by Aracena et al. (2011) looked at water column
5 productivity in response to surface sediment export production in various Chilean
6 Patagonia fjords (41-56°S). They calculated primary production rates during the summer
7 between ~35 mmol C m⁻² d⁻¹ in the more southern regions (52°S - 55°S) and ~488 C m⁻² d⁻¹
8 to the north (41°S - ~44°S). In Central Patagonia, Aracena et al. (2011) estimated
9 primary productivity at ~57 mmol C m⁻² d⁻¹ in the spring, a value comparable to some
10 seasonal estimates in Glacier Bay, and found primary production rates comparable to
11 those of Norwegian fjords (~9 to ~360 mmol C m⁻² d⁻¹).

12 There have been a number of studies conducted within Glacier Bay, though
13 conclusions of several studies are contradictory. Many of these studies had a short
14 duration and limited coverage, missing much of the spatial, seasonal, and annual
15 variability (Hooge et al, 2003). This lack of data leads to a significant gap in
16 understanding of carbon cycling in Glacier Bay, as well as a lack of predictability of
17 responses to changes in this estuarine system as climate change progresses. To capture
18 some of the seasonal and spatial variability in the bay, we collected and analyzed
19 monthly samples over a two-year period. This sampling regime, along with the variety of
20 samples taken, has provided us with the most robust dataset collected in Glacier Bay and
21 allowed us to elucidate the dynamic nature of NCP in a glaciated fjord. Our goal for this
22 study was to estimate the current level of seasonal NCP in Glacier Bay and evaluate how
23 this, along with air-sea CO₂ flux, impact the carbon dynamics in this glaciated fjord. Our

1 findings also contribute to the limited knowledge regarding carbon cycling in Glacier Bay
2 and how it is impacted by glacial runoff. Our estimates are the first attempt to assess the
3 impact of seasonal glacial melt on NCP in Glacier Bay. We wish to fill in some gaps in
4 how glacial freshwater may influence net community production within a glaciated fjord
5 ecosystem and estimate how continued glacial melt may impact productivity in Glacier
6 Bay.

8 **2.0 Background**

9 Glacier Bay was once covered by one large icefield, the Glacier Bay Icefield, that
10 has been rapidly retreating since the Industrial Revolution, scouring the bay and leaving
11 behind many alpine and tidewater glaciers. Currently, the marine portion of Glacier Bay
12 is roughly 100 km from the entrance sill to the end of the west arm, and reaches depths >
13 400 m and > 300 m in the east arm and west arm, respectively (Fig. 2).

14 Seasonal variation in factors such as light availability, turbulent or wind mixing
15 and freshwater input, impact physical conditions that are vital to primary production,
16 including stratification, photic depth, and nutrient availability. These drivers of NCP vary
17 temporally and spatially within Glacier Bay. Glacial runoff, along with glacial stream
18 input, impart freshwater into the marine system, especially along the arms of the bay.
19 Peak runoff has been shown to occur during the fall, though there is fairly constant flow
20 from June to September (Hill, 2009). Low-nutrient glacial runoff is prevalent, and while
21 it aids in stratification, its low macronutrient concentrations dilute available nutrients in
22 the northern regions nearest tidewater outflows. In the lower parts of the bay, glacial
23 influence is lower and macronutrients are more abundant allowing higher levels of

1 primary production during spring and summer. Glacier Bay maintains relatively elevated
2 phytoplankton concentrations throughout the year compared to levels observed in similar
3 Alaskan fjords (Hooge & Hooge, 2002). However, insufficient research has been done on
4 the biological system within Glacier Bay to understand why this occurs.

5 For this paper, we have calculated seasonal NCP and air-sea carbon flux for the
6 four regions within Glacier Bay in order to better understand ecosystem production in a
7 glacially dominated environment, representative of much of the southern coastal AK
8 region. This study has greatly enhanced our understanding of how glacial melt and air-
9 sea flux impacts DIC concentrations, and thus NCP, in estuaries, like Glacier Bay, which
10 are numerous along the Gulf of Alaska coast in Alaska, as well as other glaciated fjords
11 worldwide.

12

13 **3.0 Methods**

14 Ten oceanographic cruises took place aboard the National Park Service's R/V Fog
15 Lark between July 2011 and July 2012. Water column samples were collected at six
16 depths (2, 10, 30, 50, 100 m and near the bottom) at each station throughout the bay (Fig.
17 1) with a maximum depth within the west arm of ~430 m (Fig. 2). Sampling depths
18 correspond with those currently being used by the Glacier Bay long-term monitoring
19 program and determined by the USGS in the 1990s. Each 'core' station (Fig. 1) was
20 sampled during every oceanographic sampling cruise, while all 22 stations were sampled
21 during the months of July and January. "Surface" water refers to water collected from a
22 depth of 2 m unless otherwise stated. Seasonal data was calculated by averaging each
23 measured parameter at each depth for all cruises during the respective seasons. The

1 summer season consists of June, July and August, fall includes September and October;
2 winter is comprised of February and March cruises, and the spring season includes the
3 months of April and May. Data has been averaged regionally within each of the four
4 regions of the bay (lower bay, central bay, east arm, and west arm) (Fig. 1). Regional
5 boundaries were selected based on historical and ongoing research in Glacier Bay.
6 Bathymetry data (Fig. 2) was retrieved from the National Geophysical Data Center.

7 Conductivity, temperature and pressure were collected on downcasts with a
8 Seabird 19-plus CTD. Dissolved oxygen (oxygen) was sampled and processed first to
9 avoid compromising the samples by atmospheric gas exchange. Samples for oxygen
10 analysis were drawn into individual 115 ml Biological Oxygen Demand flasks and rinsed
11 with 4-5 volumes of sample, treated with 1 mL MnCl_2 and 1 mL NaI/NaOH , plugged,
12 and the neck filled with DI water to avoid atmospheric exchange. Dissolved oxygen was
13 sampled and analyzed using the Winkler titrations and the methods of Langdon (2010).
14 Samples were analyzed within 48 hours. Apparent oxygen utilization (AOU) was derived
15 from observed oxygen concentrations using Ocean Data View calculations in version
16 4.6.2 (Schlitzer, 2013).

17 DIC and total alkalinity (alkalinity) samples were drawn into 250 mL borosilicate
18 bottles. Samples were fixed with a saturated mercuric chloride solution (200 μl), the
19 bottles sealed, and stored until analysis at the Ocean Acidification Research Center at the
20 University of Alaska Fairbanks. High-quality DIC data was attained by using a highly
21 precise (0.02%; 0.4 $\mu\text{moles kg}^{-1}$) VINDTA 3C-coulometer system. Alkalinity was
22 determined by potentiometric titration with a precision of $\sim 1 \mu\text{moles kg}^{-1}$. Certified
23 reference material, prepared and distributed by Scripps Institute of Oceanography,

1 University of California, San Diego (Dr. Andrew Dickson's Laboratory), were run daily
2 before sample analysis to ensure accuracy of sample values. The VINDTA 3C provides
3 real-time corrections to DIC and alkalinity values according to in-situ temperature and
4 salinity.

5 Dissolved macronutrient samples (nitrate, phosphate, silicate) were filtered
6 through 0.8 μm Nuclepore filters using in-line polycarbonate filter holders into 25 ml
7 HDPE bottles and frozen (-20°C) until analysis at UAF. Samples were filtered to remove
8 any particles, such as glacial silt, that had the potential to clog equipment during analysis.
9 Samples were analyzed within several weeks of collection using an Alpkem Rapid Flow
10 Analyzer 300 and following the protocols of Mordy et al. (2010).

11 Particulate organic carbon (POC) samples were collected from Niskins into brown
12 1 L Nalgene bottles and stored for filtering within 2 days of collection. Samples were
13 collected at 2 m, 50 m and bottom depths. A known volume of samples was filtered
14 through muffled and preweighed 13 mm type A/E glass fiber filters using a vacuum
15 pump. Muffling involved using tweezers to wrap filters in aluminum foil and heating
16 them at 450°F for ~ 6 hours in a muffling furnace in order to remove any residual organic
17 material. Filtered samples were frozen for transport back to UAF where they were then
18 dried and reweighed. Analyses were completed by OARC at UAF and were run using the
19 methods outlined in Goñi et al. (2001).

20 The partial pressure of CO_2 ($p\text{CO}_2$) was calculated using CO2SYS (version 2.0), a
21 program that employs thermodynamic models of Lewis and Wallace (1995) to calculate
22 marine carbonate system parameters. Seasonally averaged atmospheric $p\text{CO}_2$ values
23 (μatm) were used (388.4, 388.9, 393.4, 393.8 and 391.8 for summer 2011 through

1 summer 2012, respectively and were averaged from the monthly averaged Mauna Loa
2 archive found at www.esrl.noaa.gov. For seawater $p\text{CO}_2$ calculations in CO2SYS we
3 used K_1 and K_2 constants from Mehrback et al., 1973 and refit by Dickson and Millero
4 (1987), KHSO_2 values from Dickson, the seawater pH scale, and $[\text{B}]_T$ value from
5 Uppström (1974).

6 CO_2 fluxes were calculated using seasonally averaged seawater temperature, wind
7 speed, and seawater and atmospheric $p\text{CO}_2$ data using the equation,

$$8 \quad \text{Flux} = L * (\Delta p\text{CO}_2) * k \quad (\text{Eq. 1})$$

9 where L is the solubility of CO_2 at a specified seawater temperature in $\text{mmol m}^{-3} \text{atm}^{-1}$
10 and $\Delta p\text{CO}_2$ represents the difference between seawater and atmospheric $p\text{CO}_2$ in μatm . k
11 is the steady/short-term wind parameterization in cm hr^{-1} at a specified wind speed and
12 follows the equation,

$$13 \quad k = 0.0283 * U^3 * (Sc/660)^{(-1/2)} \quad (\text{Eq. 2})$$

14 where U is wind speed in m s^{-1} , Sc is Schmidt number, or the kinematic velocity of the
15 water divided by the molecular diffusivity of a gas in water, and was normalized to 660
16 cm hr^{-1} , equivalent to the Sc for CO_2 in 20°C seawater (Wanninkhof and McGillis, 1999).
17 Wind speeds were cubed using the methods of Wanninkhof and McGillis (1999) in an
18 attempt to account for the retardation of gas transfer at low to moderate wind speeds by
19 surfactants and the bubble-enhanced gas transfer that occurs at higher wind speeds.

20 Seawater temperatures for flux calculations were taken from surface bottle CTD
21 data. Wind speeds were obtained from a Bartlett Cove, AK weather station (Station
22 BLTA2) located in Glacier Bay and maintained by the National Weather Service Alaska
23 Region.

1 NCP calculations were made using the seasonal drawdown of photosynthetic
2 reactant DIC within the mixed layer (upper 30 m) and were normalized to a salinity of
3 35. NCP production was calculated between each season from the summer of 2011 to the
4 summer of 2012 (i.e. the change in concentrations between each consecutive season)
5 according to the equation (Williams, 1993),

$$\begin{aligned} \text{NCP} &= \text{DIC}_{\text{season2}} - \text{DIC}_{\text{season1}} && \text{(Eq. 3)} \\ &= \Delta\text{DIC (moles C per unit volume area)} \end{aligned}$$

8 The influx of high-DIC waters (e.g., river discharge) can cause a dampening of the NCP
9 signal. This effect can be accounted for by normalizing DIC to a constant deep-water
10 reference salinity ($S=35$; Millero, 2008). Since this equation only reflects the effects of
11 DIC, freshwater influences on alkalinity were accounted for by correction of the seasonal
12 changes in alkalinity (Lee, 2001) using the equation,

$$\Delta\text{DIC}_{\text{Alk}} = 0.5 * (\Delta\text{Alk} + \Delta\text{NO}_3^-) \quad \text{(Eq. 4)}$$

14 and subtracting this value from the seasonal change in salinity-normalized DIC (nDIC),
15 thus providing an NCP in which the significant process influencing seasonal changes to
16 DIC concentrations is biological productivity (Bates et al, 2005; Mathis et al., 2009;
17 Cross et al., 2012). Error imparted in calculating parameters, including DIC analysis and
18 averaging of nutrient concentrations within the mixed layer, are propagated through our
19 NCP estimates at $\sim \pm 5\%$ of the final NCP calculation. Error propagated through each
20 NCP estimate is listed with the NCP calculations in Table 1.

21

22 **4.0 Caveats**

1 While seasonal water column DIC concentration changes can be a good
2 approximation to determine seasonal NCP, there are several estuarine processes that we
3 were unable to constrain that likely influenced our NCP estimates and act as additional
4 sources of uncertainty. Some other sources of uncertainty, such as the influence of glacial
5 flour, was reduced through averaging of spatial and regional parameters as stations were
6 reoccupied within ~30 days of one another.

7 Glacial flour can enhance DIC concentrations in seawater. Therefore, there is the
8 possibility that the inclusion of glacial flour may have increased our DIC concentrations
9 with respect to DIC drawdown from primary production. In this case, our estimates may
10 underestimate NCP. However, we were not able to quantify the amount of glacial flour
11 deposited in Glacier Bay or analyze its composition for this study. In Glacier Bay, the
12 influence of glacial flour is limited to the northern regions (i.e. east and west arms) that
13 are directly influence by glacial outflow, many of which enter the bay along inlets and
14 not the main arms of the bay, possibly reducing the impact of glacial flour at many
15 stations. Unfortunately, there is insufficient data to quantitatively estimate the amount
16 and makeup of glacial flour or what error it imparts into our NCP calculations, but we
17 assume for the sake of our analysis that it is relatively small.

18 Freshwater runoff that enters the bay via glacial streams flows over streambeds
19 and can leach minerals and nutrients from bedrock, enhancing these concentrations in the
20 surface waters of Glacier Bay. While stream water runoff in Glacier Bay was not
21 analyzed for this study, studies of glacial runoff in southeast Alaska have shown
22 allochthonous stream water dissolved organic carbon (DOC) to be negatively correlated
23 with glacial coverage (Hood, et al., 2009). Examining watersheds along the Gulf of

1 Alaska, Hood et al. (2009) also found that the most heavily glaciated watersheds were a
2 source of the oldest, most labile (66% bioavailable) dissolved organic matter (DOM) and
3 that increased input of glacial melt was associated with increased proportions of DOM
4 from microbial sources. As we were unable to chemically analyze glacial runoff in
5 Glacier Bay, our NCP calculations using only changes in DIC concentrations
6 underestimate NCP in the bay, though freshwater input is corrected to some degree by
7 salinity normalized DIC concentrations. The quantification of freshwater input into the
8 bay is also hindered by the lack of any active gauging stations within the bay (Hill et al.,
9 2009). Glacially-derived DOC has been shown to be highly bioavailable, though
10 inversely correlated with glacial coverage (Hood et al., 2009; Hood et al., 2015). While
11 the remineralization of highly labile DOC between station occupations could have added
12 DIC back into mixed layer and decreased the signal of seasonal drawdown, any
13 significant contribution of DIC from remineralization in the mixed layer seems unlikely
14 given the slow remineralization rates and the short time periods (~30 days) between
15 station occupations.

16 Additionally, while glacial freshwater input has been shown to have some impact
17 on NCP estimates in Greenland fjords, Meire et al. (2015) found biological processes to
18 be the main driver of carbon dynamics. In a study similar to ours in Glacier Bay, AK,
19 Meire and his team estimated air-sea CO₂ fluxes and NCP in the Godthåbsfjord system in
20 western Greenland, as well as the impact of freshwater on these estimates. They
21 identified biological processes as the most important driver of carbon dynamics,
22 accounting for 65 to 70% of the total CO₂ uptake by the fjord system (Meire et al., 2015).

1 Some literature suggests that internal waves may form within the lower bay in an
2 area of station 02, known as Sitakaday Narrows. This is an area of constriction with
3 accelerated currents that can produce hydraulic instabilities, potentially causing internal
4 waves that may influence mixing at depth as well as at a distance from this region (Hooge
5 & Hooge, 2002). These internal waves may affect nutrient replenishment to surface
6 waters, as well as mixing of DIC across the mixed layer. This addition of high-DIC
7 waters from depth may also lead to an underestimation of NCP. However, we cannot
8 make an estimation of how this affects our NCP estimations, as there is debate about how
9 often internal waves form in Glacier Bay.

10

11 **5.0 Results**

12 **5.1 Spatial and seasonal salinity distributions**

13 Salinity distributions throughout the bay were generally the result of the influence
14 of glacial runoff. During this summer season salinity ranged from 22.9 in surface waters
15 at station 20 to 32.5 in the bottom waters of station 24 in Cross Sound. Isohalines were
16 horizontal down to ~50 m from the upper arms through the upper portion of the lower
17 bay then became vertical in the lower bay, intersecting the surface just north of station 01
18 (Fig. 3).

19 Salinity was more constrained during the fall, with a full water column range
20 between 25.3 in the surface waters at station 07 and 31.4 at depth (~130 m) at station 13.
21 Similar to the previous summer, isohalines remained horizontal from the upper arms to
22 the mid-lower bay near station 01 where they become vertical and intersected the surface.

1 Salinities in the lower bay near were between ~30 and 31, with the higher salinities at
2 depth in Cross Sound.

3 During the winter salinity had a narrow range 29.6 and 31.6. The highest salinities
4 were observed in the bottom waters at station 24, though salinity was similar at all depth
5 at this station (~31.4). The lowest salinities (~30) were within the top 10 m of station 12
6 with similar surface salinities throughout both arms. In the spring, salinity continued to
7 have a narrow range, with bay-wide salinities between ~28.9 at the surface of station 12
8 and 31.7 in the bottom water of station 24. Salinities below a depth of 50 m were
9 relatively homogenous at ~31 (Fig. 3).

10 Returning to summer conditions in 2012, a strong salinity gradient was observed
11 in the upper 50 m along the east and west arms. Salinities across the bay ranged from
12 24.1 in the surface waters of station 12 to 32.2, at depth at station 24. The lowest
13 salinities were observed in the surface waters at the head of both arms, with this low
14 salinity signal stretching south through the through the central bay. Stations within the
15 lower bay had the highest salinities having salinities between ~31 and 32 at all depths.

16

17 **5.2 Spatial and seasonal distributions of DIC and nitrate**

18 DIC and nitrate are important inorganic components that are consumed during
19 photosynthesis at various rates throughout the year in Glacier Bay. DIC concentrations
20 during the summer of 2011 ranged from ~1400 to 2100 $\mu\text{mol kg}^{-1}$, with the lowest
21 concentrations in the arms and upper-central bay. Nitrate concentrations throughout the
22 water column ranged from ~2.5 to ~37 $\mu\text{mol kg}^{-1}$, with slightly less variability in the
23 surface layer (~2.5 and 24 $\mu\text{mol kg}^{-1}$). Surface nitrate concentrations were low, but

1 remained $>5 \mu\text{mol kg}^{-1}$ at all stations. While there was a large drawdown of nitrate,
2 particularly in spring and summer (as much as $20 \mu\text{mol kg}^{-1}$ when compared to winter
3 concentrations), surface waters were not depleted at any of the observed stations.

4 In the fall of 2011, DIC and nitrate concentrations increased in the surface waters,
5 with DIC ranging from $\sim 1700 \mu\text{mol kg}^{-1}$ to $2040 \mu\text{mol kg}^{-1}$, while below the surface
6 concentrations reached $\sim 2075 \mu\text{mol kg}^{-1}$. Water column nitrate concentrations were
7 between $\sim 12 \mu\text{mol kg}^{-1}$ and $32 \mu\text{mol kg}^{-1}$ with similar concentrations within surface
8 waters ($11 \mu\text{mol kg}^{-1}$ to $30 \mu\text{mol kg}^{-1}$) and the lowest concentrations observed in the arms.
9 DIC concentrations were much more constrained during the winter ($\sim 1920 \mu\text{mol kg}^{-1}$ to
10 $2075 \mu\text{mol kg}^{-1}$) than during previous seasons. Nitrate concentrations ranged from ~ 12
11 $\mu\text{mol kg}^{-1}$ to $33 \mu\text{mol kg}^{-1}$.

12 During the spring of 2012 DIC and nitrate had reduced concentrations in surface
13 waters across the bay. Surface DIC concentrations were between $\sim 1750 \mu\text{mol kg}^{-1}$ and
14 $2025 \mu\text{mol kg}^{-1}$, with water column concentrations reaching $\sim 2075 \mu\text{mol kg}^{-1}$ (Fig. 4).
15 Nitrate concentrations ranged from $\sim 7 \mu\text{mol kg}^{-1}$ to $\sim 31 \mu\text{mol kg}^{-1}$, with an observed
16 surface water maximum of $\sim 20 \mu\text{mol kg}^{-1}$. Further drawdown of DIC and nitrate in
17 surface waters was observed during the summer of 2012. However, concentrations did
18 not drop as low as was observed during the previous summer. DIC concentrations ranged
19 from ~ 1545 to $2066 \mu\text{mol kg}^{-1}$. Nitrate concentrations varied from ~ 13 to $33 \mu\text{mol kg}^{-1}$,
20 with surface concentrations between ~ 17 and $31 \mu\text{mol kg}^{-1}$. The stations with the lowest
21 DIC and nitrate concentrations were those within the east arm and west arm (Fig. 4).

22

23 **5.3 Rates and Masses of NCP**

1 The seasonal transition between the summer and fall of 2011 had the largest rates
2 of NCP observed during the year of study. Rates of NCP were positive in all regions of
3 the bay and were highest within the east and west arms of the bay at 70.3 ± 3.5 and 81.3
4 ± 4.1 mmol C m⁻² d⁻¹, respectively. A similar NCP rate of 68.9 ± 3.4 mmol C m⁻² d⁻¹ was
5 observed within the lower bay, while the central bay had the lowest rate between of 53.6
6 ± 2.7 mmol C m⁻² d⁻¹ (Table 1).

7 Calculated rates of NCP became negative between fall and winter, as well as from
8 winter to spring. Between fall and winter, the lower bay had a rate of -14.2 ± 0.7 mmol C
9 m⁻² d⁻¹ followed by the central bay at -11.5 ± 0.6 mmol C m⁻² d⁻¹. Rates of NCP were
10 negative in the east and west arms (-0.5 ± 0.03 and -1.3 ± 0.1 mmol C m⁻² d⁻¹),
11 respectively. Between the winter and spring of 2012, rates of NCP remained negative
12 within the east and west arms (-36.4 ± 1.8 mmol C m⁻² d⁻¹ and -26.6 ± 1.3 mmol C m⁻² d⁻¹,
13 respectively), and to a lesser degree in central bay (-17.5 ± 0.9 mmol C m⁻² d⁻¹). Positive
14 NCP rate was estimated for the lower bay of 17.6 ± 0.9 mmol C m⁻² d⁻¹. Between the
15 spring and summer of 2012 NCP rates were positive across the bay, with the highest rate
16 in lower bay (19.4 ± 1.0 mmol C m⁻² d⁻¹). The central bay and the east arm had rates of
17 17.2 ± 0.9 and 15.7 ± 0.8 mmol C m⁻² d⁻¹, respectively, while the west arm had a lower
18 rate at 6.0 ± 0.3 mmol C m⁻² d⁻¹.

19 The total mass (kg C d⁻¹) of carbon produced from NCP was also estimated
20 between each season (Table 1). Production occurred between the summer and fall of
21 2011, with the greatest production in the lower bay ($4.5 \times 10^5 \pm 1.3 \times 10^4$ kg C d⁻¹). The
22 central bay had a large amount of production ($2.2 \times 10^5 \pm 1.1 \times 10^4$ kg C d⁻¹), followed by
23 the west and east arms ($1.8 \times 10^5 \pm 8.8 \times 10^3$ and $7.6 \times 10^4 \pm 3.8 \times 10^3$ kg C d⁻¹ respectively).

1 Between the fall and winter the lower bay had carbon production of $-9.3 \times 10^4 \pm$
2 $4.6 \times 10^3 \text{ kg C d}^{-1}$, while the east arm had a lowest degree of production at $-5.2 \times 10^2 \pm 2.6$
3 kg C d^{-1} . NCP masses in central bay and west arm were also negative ($-4.7 \times 10^4 \pm$
4 2.3×10^4 and $-2.7 \times 10^3 \pm 1.4 \times 10^2 \text{ kg C d}^{-1}$, respectively). Between the winter and spring of
5 2012 masses in the east and west arms were estimated at $-3.9 \times 10^4 \pm 2.0 \times 10^3 \text{ kg C d}^{-1}$ and -
6 $5.8 \times 10^4 \pm 2.9 \times 10^3 \text{ kg C d}^{-1}$, respectively while the central bay had a value of $-7.1 \times 10^4 \pm$
7 $3.6 \times 10^3 \text{ kg C d}^{-1}$. The lower bay was the only region to have a positive NCP of $1.1 \times 10^5 \pm$
8 $5.7 \times 10^3 \text{ kg C d}^{-1}$.

9 Transitioning from the spring to summer the lower bay had the greatest
10 production ($1.3 \times 10^5 \pm 6.3 \times 10^3 \text{ kg C d}^{-1}$), followed by the central bay ($7.0 \times 10^4 \pm 3.5 \times 10^3$
11 kg C d^{-1}). The arms exhibited the lowest biomass production, with an NCP in the west
12 arm of $1.3 \times 10^4 \pm 6.5 \times 10^2 \text{ kg C d}^{-1}$ and $1.7 \times 10^4 \pm 8.5 \times 10^2 \text{ kg C d}^{-1}$ in the east arm.

13

14 **5.4 Spatial and seasonal distribution of POC**

15 During the summer of 2011 surface POC concentrations were between ~ 12 and
16 $\sim 55 \mu\text{mol kg}^{-1}$. Station 20 had the highest POC concentration at all sampled depths (~ 46
17 $\mu\text{mol kg}^{-1}$, ~ 30 , and $\sim 42 \mu\text{mol kg}^{-1}$, surface to bottom), while the west arm had the
18 highest POC concentrations below the surface ($\sim 33 \mu\text{mol kg}^{-1}$ at 50 m and depth). The
19 west and east arms exhibited negative AOU (~ -80 and $\sim -64 \mu\text{mol kg}^{-1}$, respectively).
20 Below the surface concentrations were similar ($\sim 9 \mu\text{mol kg}^{-1}$), while surface waters had a
21 POC concentration of $\sim 28 \mu\text{mol kg}^{-1}$. Lower bay had relatively lower POC concentrations
22 ($\sim 15 \mu\text{mol kg}^{-1}$ at all depths).

23 POC concentrations decreased, especially within surface waters during the fall. A

1 maximum regional POC concentration ($\sim 13 \mu\text{mol kg}^{-1}$) was observed in surface waters of
2 the west arm. Below the surface layer POC concentrations were low, between ~ 5 and ~ 8
3 $\mu\text{mol kg}^{-1}$. A maximum regional surface AOU ($\sim 82 \mu\text{mol kg}^{-1}$) was estimated for the
4 lower bay and a minimum ($\sim 2 \mu\text{mol kg}^{-1}$) in the surface waters of the central bay (Fig. 5).

5 In the winter of 2012 surface water POC concentrations were not found to exceed
6 $20 \mu\text{mol kg}^{-1}$ and AOU across the bay were on the order of $\sim 70 \mu\text{mol kg}^{-1}$. Surface POC
7 concentrations ranged from ~ 2 to $\sim 15 \mu\text{mol kg}^{-1}$, while POC concentrations at depth
8 varied between ~ 3 and $16 \mu\text{mol kg}^{-1}$. The regional maximum in POC was in the surface
9 waters in the west arm ($\sim 11 \mu\text{mol kg}^{-1}$). The east arm and lower bay both had maximum
10 POC concentrations in the bottom waters (~ 14 and $\sim 9 \mu\text{mol kg}^{-1}$, respectively).

11 POC concentration in the surface waters increased during the spring of 2012,
12 primarily within northern regions of the bay. The east arm had the greatest increase in
13 surface POC ($\sim 62 \mu\text{mol kg}^{-1}$) with concentrations decreasing in the surface water to the
14 south. The west arm and central bay had similar surface POC concentrations of $\sim 35 \mu\text{mol}$
15 kg^{-1} , and $\sim 30 \mu\text{mol kg}^{-1}$, respectively. The lower bay had the lowest surface POC
16 concentrations with $\sim 13 \mu\text{mol kg}^{-1}$, while having the highest rate of NCP and AOU (~ 93
17 $\mu\text{mol kg}^{-1}$). The lower bay subsurface and deepwater AOU values were positive and POC
18 concentrations, $\sim 9 \mu\text{mol kg}^{-1}$ each, were the highest among the regions.

19 AOU values decreased in surface waters across the bay, while rates of NCP were
20 elevated within these waters during the summer of 2012. Surface POC concentrations
21 were highest in the east arm ($\sim 50 \mu\text{mol kg}^{-1}$), while below the surface layer, POC
22 concentrations decreased, ranging from ~ 4.5 to $\sim 7 \mu\text{mol kg}^{-1}$ at 50 m and ~ 5 to $\sim 8 \mu\text{mol}$
23 kg^{-1} at depth. The west arm and central bay regions had surface POC concentrations of

1 ~23 $\mu\text{mol kg}^{-1}$ and the lower bay exhibited the lowest surface POC concentration with
2 ~13 $\mu\text{mol kg}^{-1}$..

3

4 **5.5 Relationship between DIC and Oxygen**

5 During the summer of 2011, oxygen concentrations ranged from ~190 to ~400
6 $\mu\text{mol kg}^{-1}$. All samples below the surface layer, as well as surface samples within the
7 lower bay followed the Redfield ratio, with concentrations at depth between ~190 and
8 280 $\mu\text{mol kg}^{-1}$ (Fig. 6). Surface samples of stations within the arms and central bay had
9 high oxygen concentrations and low DIC. Surface oxygen was higher than that at depth,
10 ranging between ~230 and 400 $\mu\text{mol kg}^{-1}$. However, in the lower bay DIC concentrations
11 remained elevated (~2030 $\mu\text{mol kg}^{-1}$) and oxygen concentrations were low (~240 μmol
12 kg^{-1}). During the fall, surface samples within the arms and central bay continued to
13 deviate from Redfield. Surface oxygen concentrations ranged from ~210 to ~330 μmol
14 kg^{-1} and corresponded with reduced surface DIC concentrations. At depth, oxygen
15 concentrations varied between ~200 and 280 $\mu\text{mol kg}^{-1}$ with C:O ratios close to Redfield.

16 All samples, at the surface and at depth, followed Redfield closely with surface
17 waters having slightly higher oxygen and lower DIC concentrations than those at depth
18 during the winter of 2012. Surface water oxygen concentrations were between 250 and
19 ~280 $\mu\text{mol kg}^{-1}$, while deeper waters ranged from ~230 to 255 $\mu\text{mol kg}^{-1}$.

20 In the spring, DIC was drawn down and oxygen concentrations increased, having
21 a range between ~270 and 410 $\mu\text{mol kg}^{-1}$. Oxygen concentrations were amplified while
22 DIC was reduced at stations in the northern-most regions of both arms. These samples
23 deviated the most from Redfield, while the remaining samples adhered to the Redfield

1 ratio. Below the surface layer, oxygen concentration throughout the bay ranged from
2 ~ 250 to $280 \mu\text{mol kg}^{-1}$

3 During the summer of 2012, the surface waters within the two arms and central
4 bay continued to diverge from Redfield. DIC concentrations within the more northern
5 regions of the bay (east arm, west arm, and central bay) were increasingly drawn down,
6 while oxygen concentrations remained elevated. Surface oxygen concentrations ranged
7 from ~ 260 to $\sim 410 \mu\text{mol kg}^{-1}$, with lower oxygen concentrations at depth, varying from
8 $200 - \sim 270 \mu\text{mol kg}^{-1}$.

9

10 **5.6 Air-Sea gas flux**

11 During the summer of 2011 winds were relatively low, at $\sim 1.6 \text{ m s}^{-1}$, with surface
12 waters of the central bay and the west arm were undersaturated with respect to
13 atmospheric CO_2 with $p\text{CO}_2$ values of $\sim 250 \mu\text{atms}$. The central bay and the west arm
14 acted as minor sinks ($\sim -0.3 \pm 0.02 \text{ mmol C m}^{-2} \text{ d}^{-1}$ each). The lower bay and east arm had
15 much higher seawater $p\text{CO}_2$ values of $\sim 488 \mu\text{atms}$ and $\sim 463 \mu\text{atms}$ and acted as sources
16 for atmospheric CO_2 of $\sim 0.2 \pm 0.01 \text{ mmol C m}^{-2} \text{ d}^{-1}$ for each region (Fig. 7).

17 During the fall of 2011, winds increased slightly to $\sim 2.0 \text{ m s}^{-1}$ and surface waters
18 in all regions of the bay were oversaturated with respect to the atmospheric CO_2 . The
19 lower bay experienced the highest $p\text{CO}_2$ at $\sim 670 \mu\text{atms}$ and acted as the largest source for
20 atmospheric CO_2 with a flux of $\sim 1.1 \pm 0.06 \text{ mmol C m}^{-2} \text{ d}^{-1}$. The central bay also had
21 elevated $p\text{CO}_2$ with $\sim 510 \mu\text{atms}$ leading to outgassing of $\sim 0.5 \pm 0.03 \text{ mmol C m}^{-2} \text{ d}^{-1}$. The
22 east arm had a $p\text{CO}_2$ and flux values similar to that of the central bay ($p\text{CO}_2 = \sim 514$
23 μatms ; flux = $\sim 0.5 \text{ mmol} \pm 0.03 \text{ C m}^{-2} \text{ d}^{-1}$). Air-sea CO_2 flux in the west arm was $\sim 0.3 \pm$

1 0.02 mmol C m⁻² d⁻¹, similar to the east arm and central bay, but had a slightly lower
2 pCO₂ of ~482 μatms (Fig. 7).

3 Surface waters during the winter of 2012 were oversaturated in CO₂ with respect
4 to the atmosphere and all regions experienced outgassing, with average wind speeds of
5 ~2.1 m s⁻¹. Regional pCO₂ values were more constrained, especially within the arms and
6 central bay, ranging from ~400 μatms in the west arm and central bay to ~432 μatms in
7 the east arm. Similar pCO₂ values and seawater temperatures (~3.5°C), led the west arm
8 and central bay to experience comparable CO₂ fluxes of ~0.03 ± 0.002 and 0.06 ± 0.003
9 mmol C m⁻² d⁻¹. The east arm had a slightly higher surface temperature (~4.1°C) and flux,
10 with ~0.18 ± 0.01 mmol C m⁻² d⁻¹, while the lower bay had a slightly higher CO₂ flux of
11 ~0.76 ± 0.04 mmol C m⁻² d⁻¹.

12 In the spring, seawater temperatures increased slightly to ~5°C across the bay
13 while salinity remained similar to winter values (~29 to 31). However, all regions except
14 for the lower bay transitioned to sinks for atmospheric CO₂. pCO₂ in the lower bay
15 remained oversaturated with respect to CO₂ at ~423 μatms and had a flux of ~0.11 ± 0.01
16 mmol C m⁻² d⁻¹. Within the other three regions of the bay, surface water temperatures
17 increased by just over 1°C. However, pCO₂ decreased in the surface waters and these
18 regions acted as sinks for atmospheric CO₂. The east arm had the greatest decrease in
19 pCO₂, dropping from ~432 μatms to ~167 μatms and exhibiting seasonal outgassing of ~
20 -0.87 ± 0.04 mmol C m⁻² d⁻¹. The central bay and west arm regions were also seasonal
21 sinks for CO₂, taking up ~ -0.39 ± 0.02 mmol C m⁻² d⁻¹ in the central bay and ~ -0.60 ±
22 0.03 mmol C m⁻² d⁻¹ in the west arm.

1 During the summer of 2012 $p\text{CO}_2$ in the east arm increased to $\sim 337 \mu\text{atms}$ with $\sim -$
2 $0.13 \pm 0.01 \text{ mmol C m}^{-2} \text{ d}^{-1}$ of ingassing. The central bay had a $p\text{CO}_2$ of $\sim 200 \mu\text{atms}$ and a
3 flux of $\sim -0.44 \pm 0.02 \text{ mmol C m}^{-2} \text{ d}^{-1}$. The lower bay and west arm, acted as sources for
4 atmospheric CO_2 , having $p\text{CO}_2$ values of $\sim 411 \mu\text{atms}$ and $\sim 507 \mu\text{atms}$, respectively, while
5 the lower bay experienced a near-neutral flux of $\sim 0.04 \pm 0.002 \text{ mmol C m}^{-2} \text{ d}^{-1}$. The west
6 arm was oversaturated with respect to atmospheric CO_2 with a $p\text{CO}_2$ of $\sim 507 \mu\text{atms}$ and a
7 flux of $\sim 0.26 \pm 0.01 \text{ mmol C m}^{-2} \text{ d}^{-1}$.

8

9 **6.0 Discussion**

10 **6.1 Relationships of DIC, Nitrate, and Dissolved Oxygen**

11 During the summer of 2011 surface waters in the arms and upper-central bay
12 deviated from Redfield ratios for C:O and C:N (Figs. 6 and 8) Waters below this surface
13 layer followed the Redfield ratios. Nitrate and phosphate concentrations in the surface
14 waters were not observed to reach depletion during the summer, indicating that they were
15 being continuously supplied to the surface layer and that phosphate (data not shown) was
16 not limiting. Sustained nutrient concentrations and nutrient replenishment may be the
17 result of physical interactions within the bay, including wind, tidal and internal wave
18 mixing, and mixing across sills.

19 Increases in oxygen and the reduction in macronutrient concentrations, including
20 DIC, within the more northern arms of the bay was due to primary production coupled
21 with the influence of glacier runoff and salinity-driven stratification limiting mixing and
22 nutrient replenishment in the mixed layer. In the fall of 2011, DIC and nitrate
23 concentrations increased while oxygen decreased in the surface waters as primary
24 production slowed and wind mixing increased. Due to decreasing primary production

1 nutrient concentrations were similar within surface waters with the lowest concentrations
2 observed in the arms where glacial runoff was still impacting surface waters. Surface
3 water ratios for C:O and C:N deviated from the Redfield ratios, but less so than observed
4 during summer as primary production began to decrease during the fall (Figs. 6 and 8).
5 During the winter of 2012, increased wind mixing and the reduction of glacial input led
6 to deeper water column mixing, with much more constrained DIC and nitrate
7 concentrations. During the winter nitrate and DIC concentrations continued to increase,
8 with C:O and C:N Redfield ratios indicated a decrease in primary production and
9 increase in mixing (Figs. 6 and 8). While DIC and nitrate concentrations fell near the
10 Redfield ratio, they deviated slightly from Redfield at the highest nitrate concentrations
11 (Fig. 4). This may have been due to nitrification of ammonium by bacteria leading to an
12 increase the nitrate concentration. Another possibility is ‘carbon overconsumption’, the
13 process in which more DIC is taken up than that inferred from the C:N Redfield ratio
14 (Voss et al., 2011). Explanations for carbon overconsumption include the preferential
15 remineralization of organic nitrogen (Thomas and Schneider, 1999) or an increased
16 release of dissolved organic carbon (Engel, et al., 2002; Schartau et al., 2007).

17 As temperatures began to warm in the spring of 2012, the onset of glacial melt
18 and primary production reduced DIC and nitrate, while increasing oxygen concentrations
19 in surface waters across the bay. DIC and nitrate correlated closely with the Redfield
20 ratio except for two surface samples located at the northernmost ends of each arm (Fig.
21 8). This deviation may be explained by the fact that these stations were the first to be
22 influenced by glacial runoff during the onset of the glacial melt season.

23 Further reduction in DIC and nitrate concentrations in surface waters was

1 observed during the summer of 2012 as primary production intensified, increasing
2 oxygen concentrations. Low nutrient glacial runoff was highest at this time of year,
3 affecting surface water DIC and nitrate concentrations within the arms. However,
4 concentrations did not drop as low as was observed during the previous summer.
5 Macronutrients did not reach depletion during the summer of 2012, implying they were
6 not the limiting primary productivity, possibly due to nutrient replenishment via tidal
7 pumping. Surface nitrate concentration continued to deviate from the C:N Redfield ratio
8 as these macronutrients were increasingly drawn down by primary productivity and
9 diluted by glacier runoff (Fig. 8). Surface waters in several regions also deviated from the
10 C:O Redfield ratio (Fig. 6) and those most affected were within the east arm and west
11 arm, as well as upper central bay, where freshwater influence was greatest. Mixing of
12 nutrient-rich marine waters from the Gulf of Alaska likely offset much of the drawdown
13 from primary production and allowed these surface waters within the lower bay to fall
14 closer to the Redfield ratio.

15

16 **6.2 NCP**

17 The seasonal transition between the summer and fall of 2011 had the largest rates
18 of NCP observed during the year of study. During this time all NCP rates were positive,
19 signifying enhanced primary productivity in the mixed layer. Rates of NCP became
20 negative during the seasonal transitions from fall to winter, as well as from winter to
21 spring. These negative NCP values indicate that air-sea fluxes (discussed in Section 5.6)
22 and organic matter respiration were prominent, increasing CO₂ (DIC) concentrations in
23 the surface waters and overwhelming any weaker signal from primary production.

1 Between the fall and winter, the lower bay experienced the highest degree of CO₂ flux
2 when compared to biological production. The biological production was overwhelmed by
3 CO₂ influx in the east and west arms, but to a less degree than in regions to the south.

4 Between the winter and spring of 2012 the lower bay was the only region where
5 biological production dominated the CO₂ flux with a positive NCP rate, reflecting the
6 region's nutrient-rich marine influence from the Gulf of Alaska. The CO₂ flux signal
7 exceeded NCP within the east and west arms of the bay and, to a lesser extent, the central
8 bay. Transition from the spring to summer of 2012, primary production was evident in
9 the NCP rates. The west arm experienced a lower rate of NCP, possibly the result of the
10 strong low-macronutrient glacial influences along the arm, which may work to hinder
11 production. Additionally, large volumes of glacial flour imparted into the surface waters
12 from runoff during summer may have limited the photic depth and thus impeded some
13 productivity in the upper arms of the bay.

14 The total mass of carbon produced between seasons via NCP was also estimated
15 (Table 1). Between the summer and fall of 2011, we observed the greatest production of
16 organic carbon of any seasonal transition, with the largest production signal in the lower
17 bay and decreasing to the north as glacial influence increased. Elevated production
18 estimates within the lower could be due to continued nutrient replenishment to surface
19 waters as a result of mixing with the more marine waters outside of the bay.

20 Despite all regions of the bay being dominated by air-sea CO₂ flux during the fall
21 and winter seasons (Table 1) there was a substantial contrast in magnitudes of estimates
22 between the marine-dominated lower bay and the glacially-influenced east arm. These
23 differences in magnitude were likely the result of a higher degree of wind and tidal

1 mixing at stations outside of and near the mouth of the bay, allowing this region to have
2 elevated air-sea flux when compared to the east and west arms (Fig. 7).

3 The production signal within the arms and central regions of the bay continued to
4 be overwhelmed by air-sea flux between the winter and spring of 2012 (Table 1). While
5 production estimates remained negative in the northern regions of the bay, the lower bay
6 had a positive NCP mass signifying increased primary production and a decrease in air-
7 sea flux in this region. This increase in NCP in the lower bay may be been the result of
8 earlier nutrient replenishment via the more marine waters outside of the bay. Between the
9 spring and summer there was increased production across the bay as stratification
10 strengthen and the hours of daylight increased, with the largest production estimates in
11 the lower bay. The east and west arms exhibited the lowest biomass production, likely
12 hindered by the inundation of low-nutrient glacial runoff that formed a fresh surface layer
13 and imparted glacial flour into the surface waters in these regions.

14

15 **6.3 Air-Sea Flux**

16 Aside from primary production, air-sea carbon dioxide (CO₂) flux also impacts
17 carbon concentrations within surface waters. In Glacier Bay, air-sea fluxes varied
18 regionally and seasonally between the summer of 2011 and the summer of 2012. During
19 the summer of 2011 winds were relatively low, reducing turbulent mixing, allowing for
20 stratification and, thus, primary production. Surface waters in the lower bay and east arm
21 acted as sources for atmospheric CO₂, while the central bay and the west arm acted as
22 sinks (Fig. 7). Drawdown of CO₂ in the west arm may be attributed to primary
23 production, as well as the influx of low nutrient glacial melt. The central bay has been
24 noted to have elevated production levels (Hooge and Hooge, 2002) that may account for

1 the drawdown of DIC and the region's sink status. Within the east arm seawater
2 temperatures were high, increasing the $p\text{CO}_2$ of these waters and, combined with
3 influence of the reduced alkalinity concentrations, resulted in an oversaturation of CO_2 in
4 the seawater with respect to the atmosphere, overwhelming any effect from DIC
5 drawdown via primary production and making this region a source for atmospheric CO_2 .
6 Turbulent mixing across and outside the sill, as well as through Sitakaday Narrows, likely
7 reduced stratification and enhanced air-sea flux, causing this region to be a source for
8 atmospheric CO_2 .

9 In the fall of 2011, winds increased slightly and all surface waters across the bay
10 experienced oversaturation with respect to the atmospheric CO_2 , with the lower bay
11 acting as the strongest regional source (Fig. 7). The high $p\text{CO}_2$ values observed during
12 fall, despite strong DIC drawdown during summer, may be the result of a variety of
13 interactions. Reduced glacial runoff during fall increased alkalinity concentrations
14 (Reisdorph and Mathis, 2014) and surface water temperatures declined allowing them to
15 hold more CO_2 while mixing brought DIC-rich waters from depth to the surface.
16 Increased winds also likely led to enhanced turbulent mixing across the bay.

17 During the winter of 2012 surface waters across all regions of the bay continued
18 to experience outgassing (Fig. 7), though to a lesser degree than during fall. The lower
19 bay experienced the largest degree of outgassing, likely due to its more turbulent mixing
20 than other regions. Despite winter having the lowest seawater temperatures, wind mixing
21 peaked and likely allowed for CO_2 -rich waters from depth and the air to enter the surface
22 waters, increasing $p\text{CO}_2$ in all regions of the bay.

1 Several regions of Glacier Bay transitioned to sinks for atmospheric CO₂ during
2 the spring of 2012 as primary production increased and winds slowed. The lower bay was
3 the exception, remaining oversaturated with respect to CO₂ and continuing to act as a
4 minor source for atmospheric CO₂. In the more northern regions, surface waters
5 experienced a slight increase in surface temperatures, but due to the onset of spring
6 productivity DIC was drawn down in the surface waters, decreasing the *p*CO₂ and
7 allowing them to become sinks for atmospheric CO₂. The east arm experienced the
8 largest decrease in *p*CO₂ and became the largest sink region within the bay, while the
9 west arm and central bay underwent similar flux transitions as primary production
10 increased, drawing down DIC in the surface waters. Within the arms, the onset of glacial
11 melt may have aided in setting up stratification, also helping to lead to larger sink statuses
12 within these regions.

13 During the summer of 2012, waters in the northern regions became increasingly
14 saturated with respect to atmospheric CO₂. While, *p*CO₂ in the east arm did increase from
15 spring values, perhaps due to a small increase in surface water temperatures and
16 reductions in alkalinity from glacial runoff, it was still undersaturated with respect to
17 atmospheric *p*CO₂. Atmospheric CO₂ uptake within the central bay strengthened slightly
18 from spring as *p*CO₂ in this region decreased, likely due to high levels of primary
19 production in this region, as well as high nutrient replenishment from tidal mixing
20 between the waters of lower bay and the stratified waters within the central bay (Hooge
21 & Hooge, 2002). Conversely, the lower bay remained a minimal source for atmospheric
22 CO₂, while the west arm transitioned into source during the summer. The lower bay
23 experiences the highest degree of turbulent or tidal mixing across the sill, within Cross

1 Sounds, and through Sitakaday Narrows, inhibiting stratification and primary production
2 and causing it act as a source for atmospheric CO₂ year-round. The difference in the
3 sink/source status of the east and west arms of the bay was likely the result of differences
4 in glacial influences, with the west arm more influenced by low-alkalinity glacial runoff
5 as it has the majority of the tidewater glaciers along its length. These glaciers caused a
6 higher degree of alkalinity and DIC dilution than was observed within the west arm.

7

8 **7.0 Conclusions**

9 Glacier Bay experiences a high degree of spatial and temporal throughout the
10 year. Environmental influences vary seasonally along a gradient from the glacially-
11 influenced northern regions within the arms to the marine-influenced lower bay. This
12 imparts spatial differences in stratification and macronutrient availability that effect
13 biological processes and thus, rates of NCP. Despite Glacier Bay's limited exchange with
14 the marine waters of the Gulf of Alaska, it has been observed to support elevated primary
15 production through most of the year (Hooge & Hooge, 2002). However, rapid
16 deglaciation within Glacier Bay has imparted a high volume of fresh glacial runoff, a
17 portion of which has been from tidewater glaciers that melt directly into the bay,
18 affecting stratification, macronutrient concentrations and influencing air-sea CO₂
19 exchange and net community production. For this study, we calculated rates of NCP and
20 air-sea CO₂ exchange in each of the four regions of Glacier Bay in order to assess current
21 production levels in the bay and how these processes may impact the carbon dynamics.
22 To date, there are no NCP or air-sea flux estimates for Glacier Bay or similar
23 southeastern Alaska fjords, despite playing an important role in the global carbon cycle.

1 Rates of NCP were positive across the bay between the summer and fall of 2011,
2 as well as between the spring and summer of 2012 during peak times of primary
3 production. NCP was highest during the transition between summer and fall of 2011,
4 with regional NCP rates ranging from ~54 to ~80 mmol C m⁻² d⁻¹. Rates during the
5 summer of 2012 were lower, between ~6 and ~20 mmol C m⁻² d⁻¹.

6 Between the fall of 2011 and winter of 2012, as well as between the winter and
7 spring of 2012, air-sea gas exchange overwhelmed any production signal across the bay,
8 especially during the fall (Fig. 7; Table 1). The one exception was lower bay between
9 winter and spring where NCP rates were positive, likely due to earlier replenishment of
10 nutrients from marine waters outside the bay.

11 The impact of rapid deglaciation in Glacier Bay can be observed in the seasonal
12 impacts on the carbon cycling and NCP in this estuarine system. This study enhances the
13 limited biogeochemical literature regarding Glacier Bay and includes one of the more
14 robust datasets from Glacier Bay. We found the highest level of NCP to occur between
15 the summer and fall seasons in 2011, with the greatest production within the glacially-
16 influenced arms of the bay. The influence of the surrounding glaciers has the potential to
17 significantly impact the efficiency and makeup of the marine food web within Glacier
18 Bay in unknown ways with unknown consequences. However, additional study of these
19 influences and their effects on the rate of NCP is needed to fully understand the impacts
20 of future deglaciation.

21

22 **Acknowledgments**

23 Thanks to the National Park Service for supporting this work through grant number

1 G7224 to the University of Alaska Fairbanks. We would also like to thank Lewis
2 Sharman, Natalie Monacci, Kristen Shake, Seth Danielson and the entire NPS staff in
3 Gustavus and Juneau, AK for their help in sample collection, logistics and editing. We
4 also want to thank the staff and visitors of Glacier Bay National Park and Preserve, as
5 well as the community of Gustavus for their support and interest in this project.

6

7

8

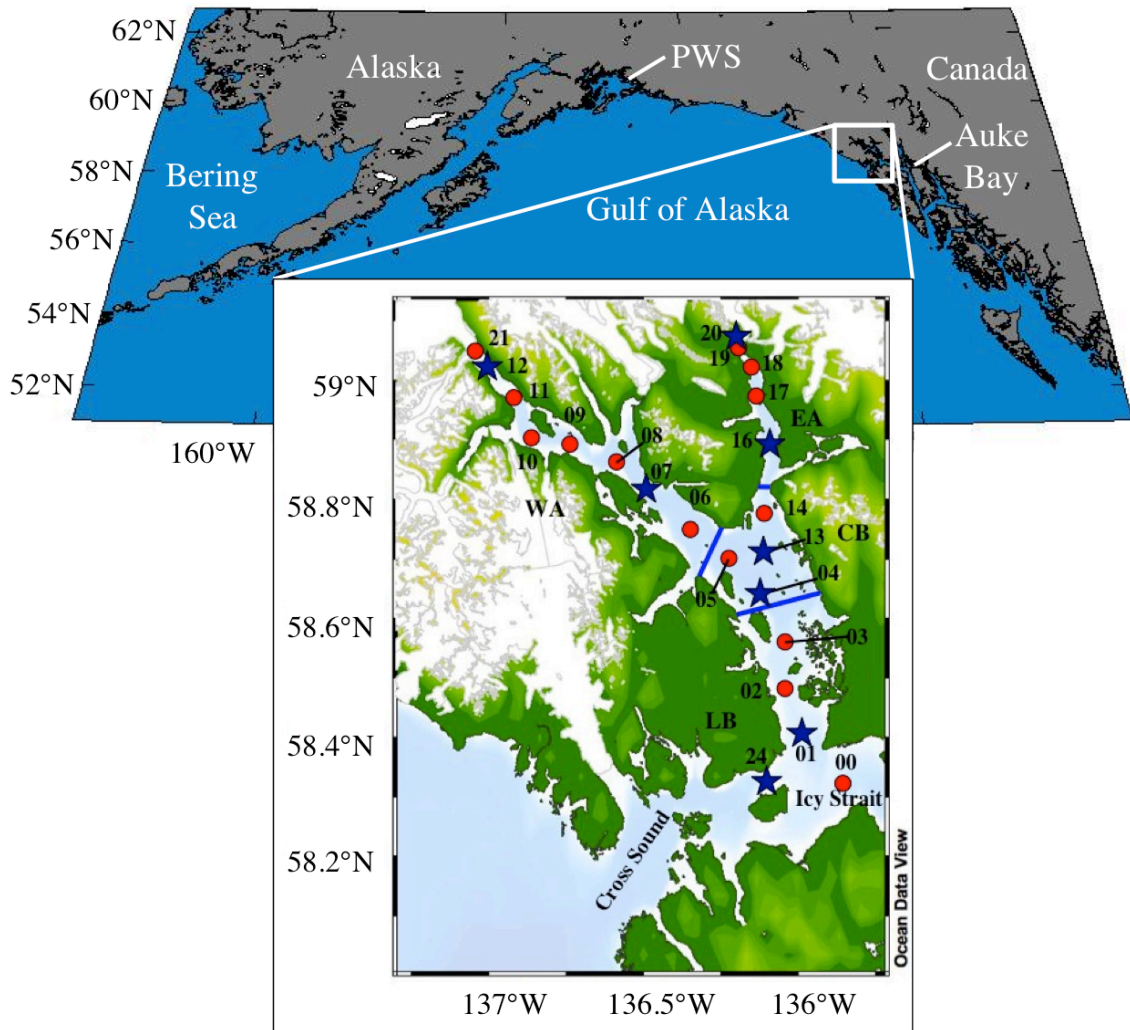
9 **References**

- 10 Anderson, L.A., Sarmiento, J.L., 1994. Redfield ratios of remineralization determined by
11 nutrient data analysis. *Global Biogeochem. Cycles* 8, 65–80.
12
- 13 Aracena, C., Lange, C.B., Luis Iriarte, J., Rebolledo, L., Pantoja, S., 2011. Latitudinal
14 patterns of export production recorded in surface sediments of the Chilean
15 Patagonian fjords (41–55°S) as a response to water column productivity. *Cont. Shelf*
16 *Res.* 31, 340–355. doi:10.1016/j.csr.2010.08.008
17
- 18 Bates, N.R., Best, M.H.P., Hansell, D. A., 2005. Spatio-temporal distribution of dissolved
19 inorganic carbon and net community production in the Chukchi and Beaufort Seas.
20 *Deep Sea Res. Part II Top. Stud. Oceanogr.* 52, 3303–3323.
21 doi:10.1016/j.dsr2.2005.10.005
22
- 23 Cross, J.N., Mathis, J.T., Bates, N.R., 2012. Hydrographic controls on net community
24 production and total organic carbon distributions in the eastern Bering Sea. *Deep*
25 *Sea Res. Part II Top. Stud. Oceanogr.* 65-70, 98–109.
26 doi:10.1016/j.dsr2.2012.02.003
27
- 28 Dickson, A.G., 1990. Standard potential of the reaction: $\text{AgCl}_{(s)} + \frac{1}{2}\text{H}_{2(g)} = \text{Ag}_{(s)} + \text{HCl}_{(aq)}$,
29 and the standard acidity constant of the ion HSO_4^- in synthetic seawater from
30 273.15 to 318.15. *The Journal of Chemical Thermodynamics*, 22, 113–127.
31 doi:10.1016/0021- 9614(90)90074-Z
32
- 33 Dickson, A.G., Millero, F.J., 1987. A comparison of the equilibrium constants for the
34 dissociation of carbonic acid in seawater media. *Deep Sea Research*, 34: 1733–
35 1743. doi:10.1016/0198-0149(87)90021-5
36

- 1 Engel, A., Goldthwait, S., Passow, U., Alldredge, A., 2002. Temporal decoupling of
2 carbon and nitrogen dynamics in a mesocosm diatom bloom. *Limnol. Oceanogr.* 47,
3 753–761. doi:10.4319/lo.2002.47.3.0753
4
- 5 Goñi, M. A., Teixeira, M.J., Perkey, D.W., 2003. Sources and distribution of organic
6 matter in a river-dominated estuary (Winyah Bay, SC, USA). *Estuar. Coast. Shelf*
7 *Sci.* 57, 1023–1048. doi:10.1016/S0272-7714(03)00008-8
8
- 9 Hill S.J. Ciavola, L. Etherington, M.J. Klaar, D.F., 2009. Estimation of freshwater runoff
10 into Glacier Bay, Alaska and incorporation into a tidal circulation model. *Estuar.*
11 *Coast. Shelf Sci.* 82, 95–107.
12
- 13 Hood, E., Fellman, J., Spencer, R.G.M., Hernes, P.J., Edwards, R., D’Amore, D., Scott,
14 D., 2009. Glaciers as a source of ancient and labile organic matter to the marine
15 environment. *Nature.* 426, 1044–1048.
16
- 17 Hood, E., Battin, T., Fellman, J., O’Neel, S., Spencer, R.G.M., 2015. Storage and release
18 of organic carbon from glaciers and ice sheets. *Nature Geosciences.* 8, 91-96.
19
- 20 Hooge, E. R., Hooge, P.N., 2002. Fjord oceanographic processes in Glacier Bay, Alaska,
21 Glacier Bay Report. Gustavus, AK.
22
- 23 Hooge, P.N., Hooge, E.R., Solomon, E.K., Dezan, C.L., Dick, C.A., Mondragon, J.,
24 Reiden, H.S., Etherington, L.L., 2003. Fjord oceanography monitoring handbook:
25 Glacier Bay, Alaska. *U.S Geol. Surv.* 1–75.
26
- 27 Langdon, C., 2010. Determination of dissolved oxygen in seawater by Winkler titration
28 using the amperometric technique. *GO-SHIP Repeat Hydrogr. Manual: A Collection*
29 *of Expert Reports & Guidelines.* 14, 1–18.
30
- 31 Lee, K., 2001. Global net community production estimated from the annual cycle of
32 surface water total dissolved inorganic carbon. *Limnol. Oceanogr.* 46, 1287–1297.
33 doi:10.4319/lo.2001.46.6.1287
34
- 35 Lewis, E., Wallace D.W.R., 1998. *CO2SYS – program developed for CO₂ system*
36 *calculations*, Report ORNL/CDIAC-105 (Carbon Dioxide Information and Analysis
37 Centre), Oak Ridge National Lab., U.S. Department of Energy.
38
- 39 Mathis, J.T., Bates, N.R., Hansell, D. A., Babila, T., 2009. Net community production in
40 the northeastern Chukchi Sea. *Deep Sea Res. Part II Top. Stud. Oceanogr.* 56, 1213–
41 1222. doi:10.1016/j.dsr2.2008.10.017
42
- 43 Mathis, J.T. and Questel, J.M., 2013. The impacts of primary production and respiration
44 on the marine carbonate system in the Western Arctic: implications for CO₂ fluxes
45 and ocean acidification. *Cont. Shelf Res.* 67, 42-51. doi: 10.1016/j.csr.2013.04.041
46

- 1 Mehrbach, C., Culberson, C.H., Hawley, J.E., Pytkowicz, R.M., 1973. Measurement of
2 the apparent dissociation constants of carbonic acid in seawater at atmospheric
3 pressure. *Limnology and Oceanography*, 18: 897–907.
4
- 5 Meire, L., Sjøgaard, D.H., Mortensen, J., Meysman, F.J.R., Soetaert, K., Arendt, K.E.,
6 Juul-Pedersen, T., Blicher, M.E., Rysgaard, S., 2015. Glacial meltwater and primary
7 production are drivers of strong CO₂ in fjord and coastal waters adjacent to the
8 Greenland Ice Sheet. *Biogeosciences*, 12, 2347–2363.
9
- 10 Mordy, C.W., Eisner, L.B., Proctor, P., Stabeno, P., Devol, A.H., Shull, D.H., Napp,
11 J.M., Whitlege, T., 2010. Temporary uncoupling of the marine nitrogen cycle:
12 accumulation of nitrite on the Bering Sea shelf. *Mar. Chem.* 121, 157–166.
13 doi:10.1016/j.marchem.2010.04.004
14
- 15 Reisdorph, S.C., Mathis, J.T., 2014. The dynamic controls on carbonate mineral
16 saturation states and ocean acidification in a glacially dominated estuary. *Estuar.
17 Coast. Shelf Sci.* 144, 8–18.
18
- 19 Schartau, M., Engel, A., Schroter, J., Thoms, S., Volker, C., Wolf-Gladrow, D., 2007.
20 Modelling carbon overconsumption and the formation of extracellular particulate
21 organic carbon. *Biogeosciences Discuss.* 4, 13–67.
22
- 23 Schlitzer, R., 2013. Ocean Data View, <http://odv.awi.de>.
24
- 25 Thomas, H., Schneider, B., 1999. The seasonal cycle of carbon dioxide in Baltic Sea
26 surface waters. *J. Mar. Syst.*, 22, 53–67.
27
- 28 Uppström, L.R., 1974. The boron/chlorinity ratio of deep-sea water from the Pacific
29 Ocean. *Deep Sea Res.*, 21, 161–162. doi:10.1016/0011-7471(74)90074-6
30
- 31 Voss, M., Baker, A., Bange, H.W., Conley, D., Cornell, S., Deutsch, B., Engel, A.,
32 Ganeshram, R., Garnier, J., Heiskanen, A.S., Jickells, T., Lancelot, C., Mcquatters-
33 Gollop, A., Middelburg, J., Schiedek, D., Slomp, C.P., Conley, D.P., 2011. Nitrogen
34 processes in coastal and marine ecosystems, in: Sutton, M.A., Howard, C.M.,
35 Erisman, J.W., Billen, G., Bleeker, A., Grennfelt, P., van Grinsven, H., Grizzetti, B.
36 (Eds.), *The European Nitrogen Assessment*. Cambridge University Press, New
37 York, pp. 147–176.
38
- 39 Wanninkhof, R., McGillis, W.R., 1999. A cubic relationship between air-sea CO₂
40 exchange and wind speed. *Geoph* 26, 1889–1892.
41
- 42 Williams, P.J., 1993. On the definition of plankton production terms: edited by: Li,
43 W.K.W. and Maestrini, S.Y., *Measurements of primary production from the
44 molecular to the global scale. ICES Mar. Sci. Symp.* 197, 9-19.
45

1 **Figures and Tables**



2

3 Fig. 1: Glacier Bay location and oceanographic sampling station map - Blue lines denote

4 regional boundaries. Red dots show all oceanographic station locations with station

5 number. Blue stars represent 'core' station location. lower bay, central bay, east, west

6 arm.

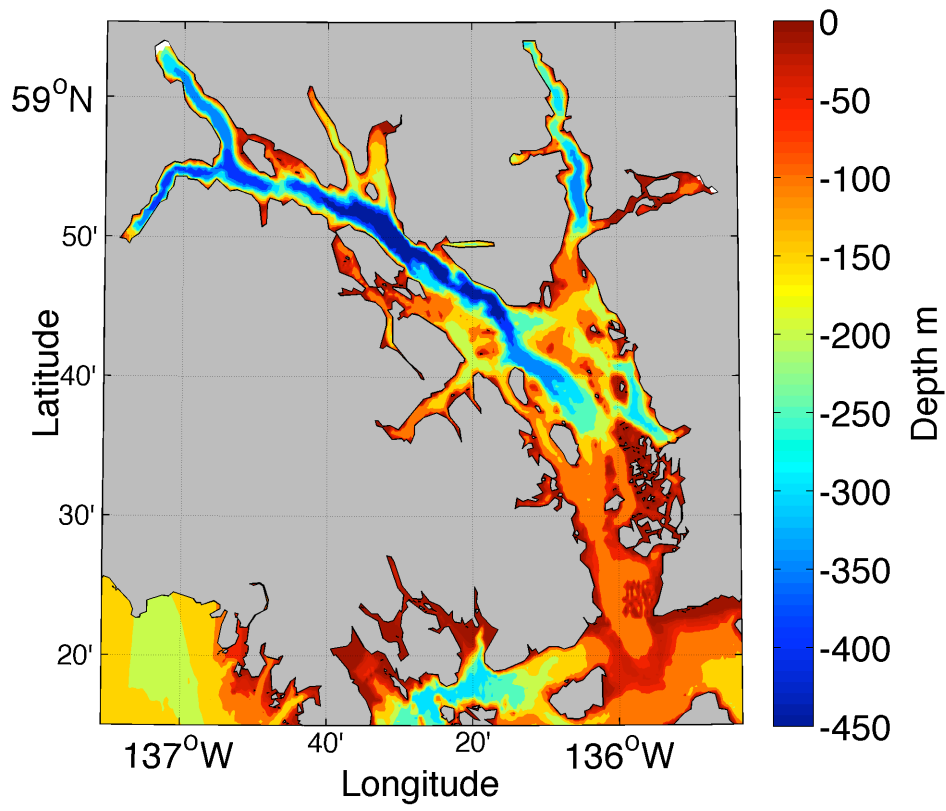
7

8

9

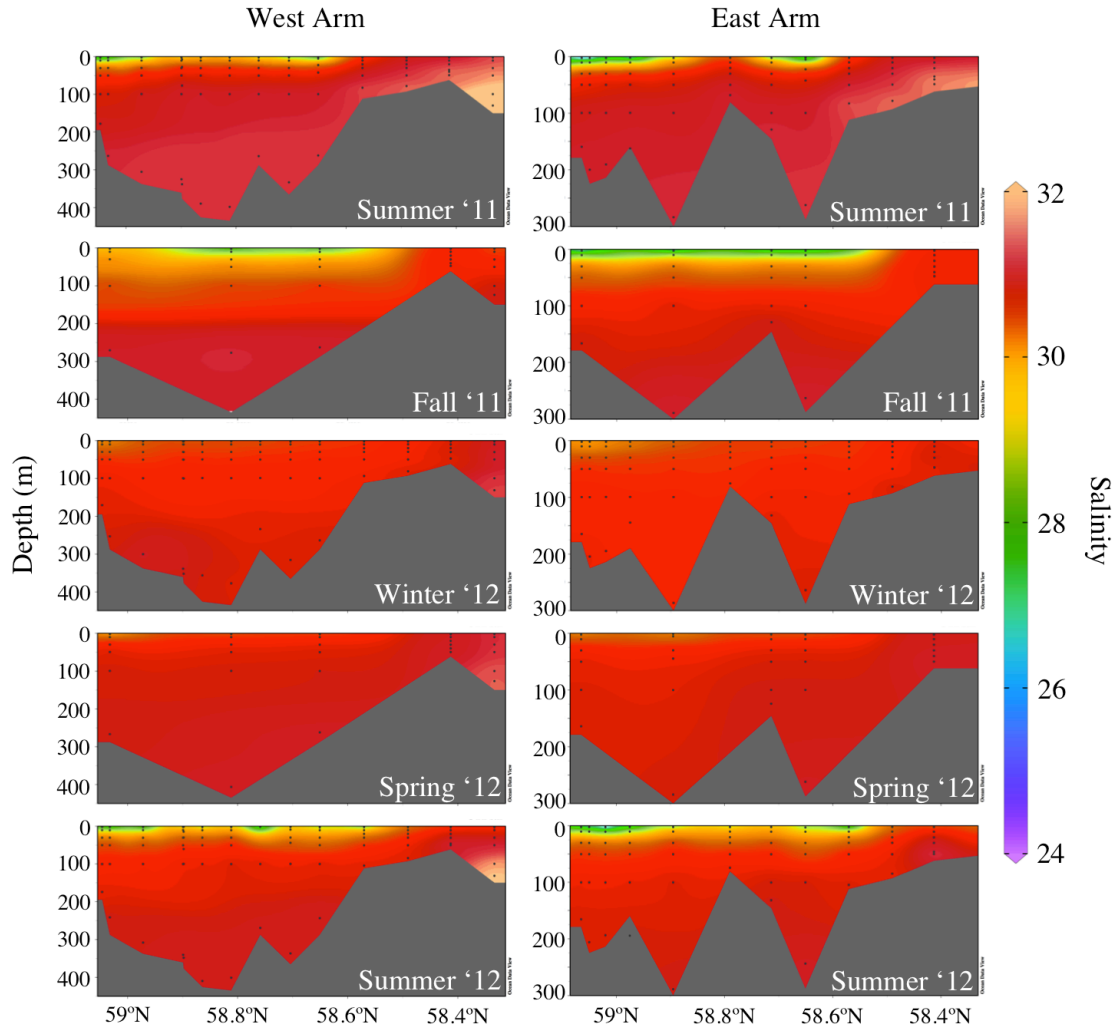
10

1



2

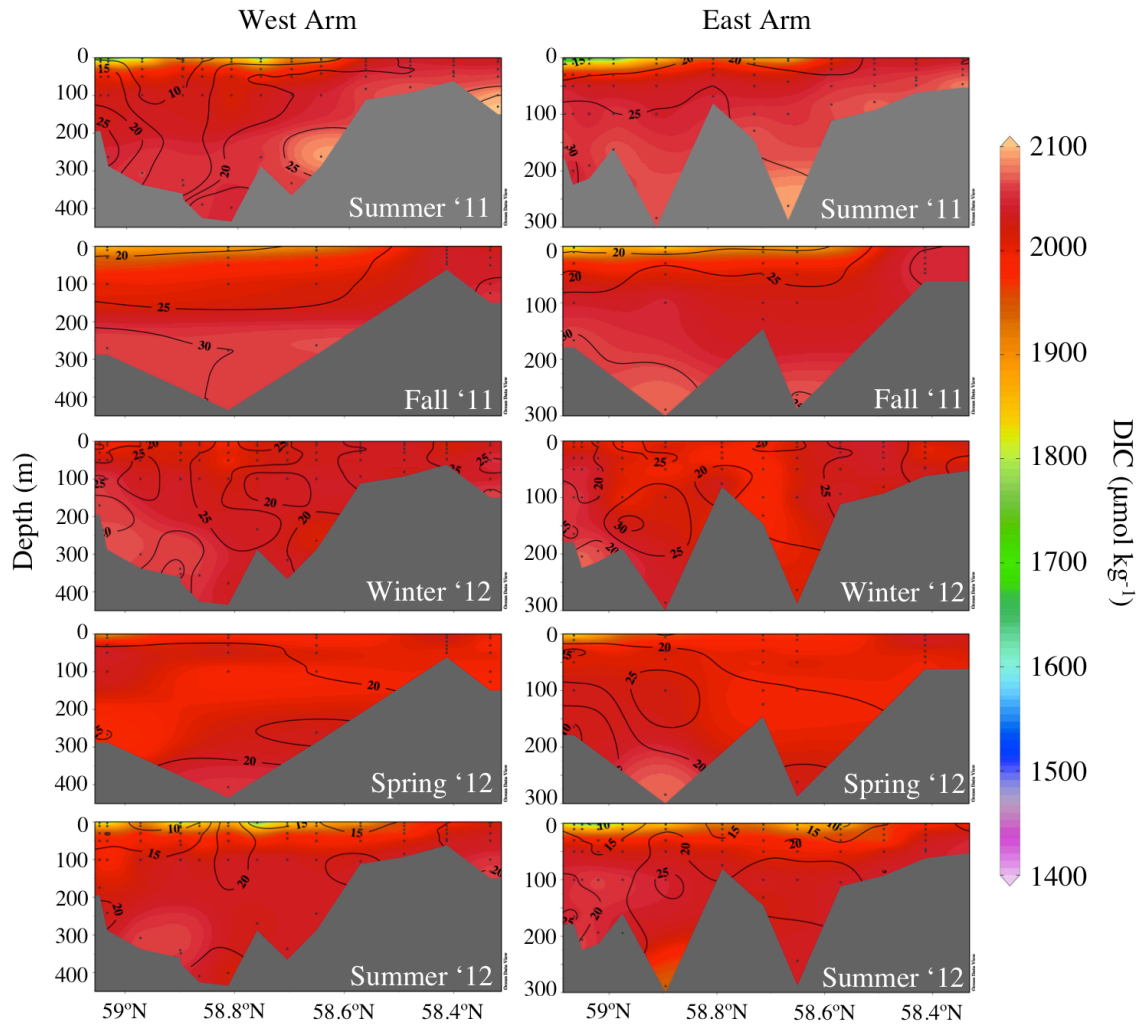
3 Figure 2: Bathymetry of Glacier Bay – Bathymetric map of Glacier Bay



1

2 Figure 3: Seasonal distribution of salinity. Spatial and seasonal distribution of salinity in
 3 the water column.

4



1

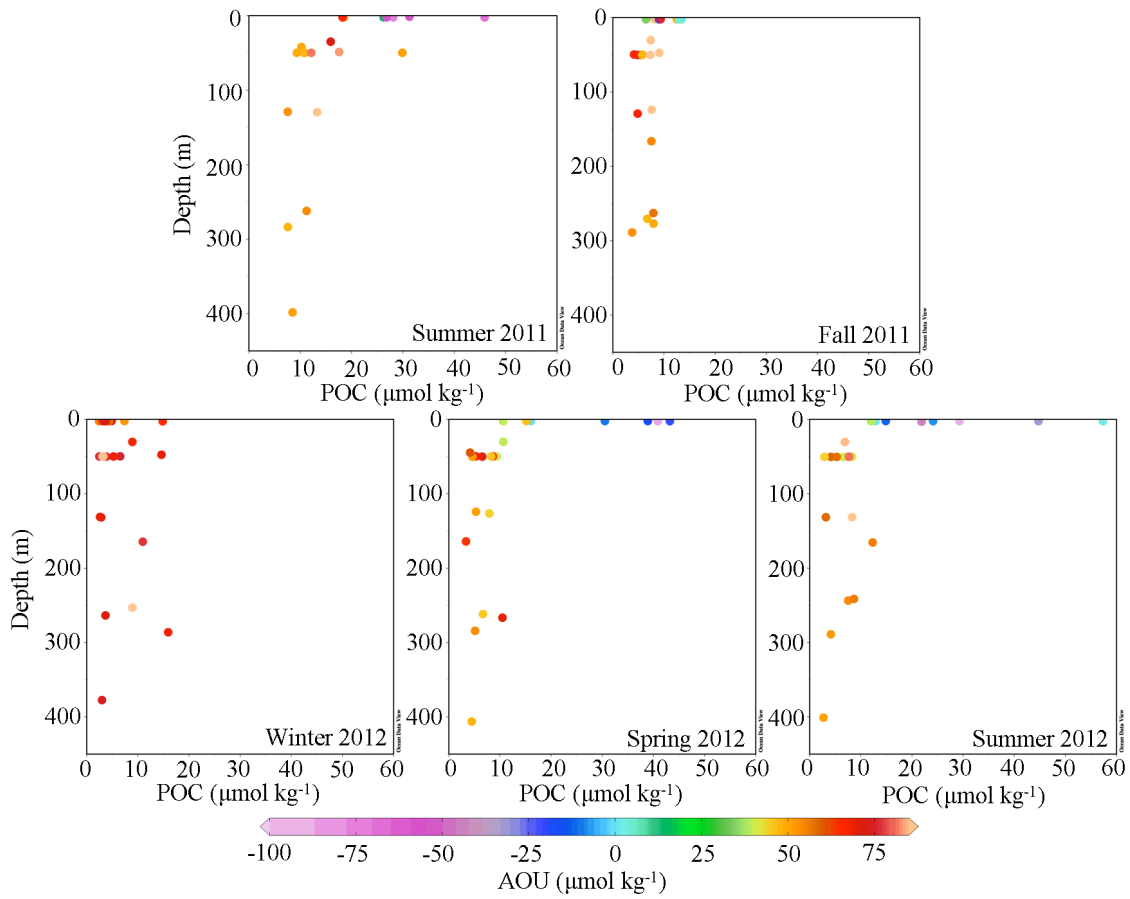
2 Figure 4: Spatial distribution of DIC and nitrate. Spatial and seasonal distribution of DIC
 3 in the water column. Contours represent nitrate concentrations

Seasonal transition	Region	Regional Area (m ²)	NCP rate (mmol C m ⁻² d ⁻¹)	NCP mass (kg C d ⁻¹)
Summer and Fall	Lower Bay	5.44x10 ⁸	68.9 ± 3.5	4.5x10 ⁵ ± 2.3x10 ⁴
	Central Bay	3.40x10 ⁸	53.6 ± 2.7	2.2x10 ⁵ ± 1.1x10 ⁴
	West Arm	1.80x10 ⁸	81.3 ± 4.1	1.8x10 ⁵ ± 8.8x10 ³
	East Arm	9.00x10 ⁷	70.3 ± 3.5	7.6x10 ⁴ ± 3.8x10 ³
Fall and Winter	Lower Bay	5.44x10 ⁸	-14.2 ± 0.7	-9.3x10 ⁴ ± 4.6x10 ³
	Central Bay	3.40x10 ⁸	-11.5 ± 0.6	-4.7x10 ⁴ ± 2.3x10 ³
	West Arm	1.80x10 ⁸	-1.3 ± 0.1	-2.7x10 ³ ± 135.7
	East Arm	9.00x10 ⁷	-0.5 ± 0.0	-515.7 ± 25.8
Winter and Spring	Lower Bay	5.44x10 ⁸	17.6 ± 0.9	1.1x10 ⁵ ± 5.7x10 ³
	Central Bay	3.40x10 ⁸	-17.5 ± 0.9	-7.1x10 ⁴ ± 3.6x10 ³
	West Arm	1.80x10 ⁸	-26.6 ± 1.3	-5.7x10 ⁴ ± 2.9x10 ³
	East Arm	9.00x10 ⁷	-36.4 ± 1.8	-3.9x10 ⁴ ± 2.0x10 ³
Spring and Summer	Lower Bay	5.44x10 ⁸	19.4 ± 1.0	1.3x10 ⁵ ± 6.3x10 ³
	Central Bay	3.40x10 ⁸	17.2 ± 0.9	7.0x10 ⁴ ± 3.5x10 ³
	West Arm	1.80x10 ⁸	6.0 ± 0.3	1.3x10 ⁴ ± 652.1
	East Arm	9.00x10 ⁷	15.7 ± 0.8	1.7x10 ⁴ ± 846.9

1

2 Table 1: Regional rates and masses of NCP – NCP by region in Glacier Bay based the
3 change in salinity-normalized DIC concentrations between seasons.

1



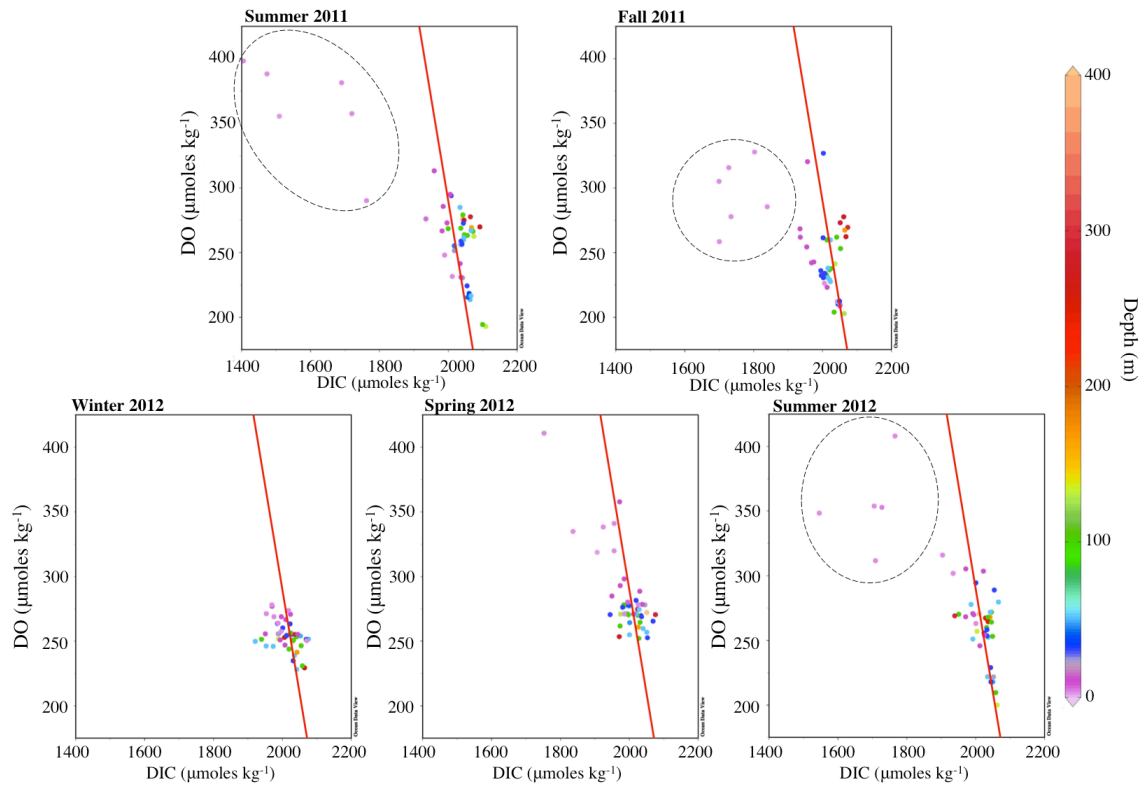
2

3 Fig. 5: Seasonal POC vs. depth vs. AOU - Seasonal scatter plots of POC concentrations

4 vs. depth for each season between the summer of 2011 through the summer of 2012.

5 Color bar represents AOU in $\mu\text{mol kg}^{-1}$.

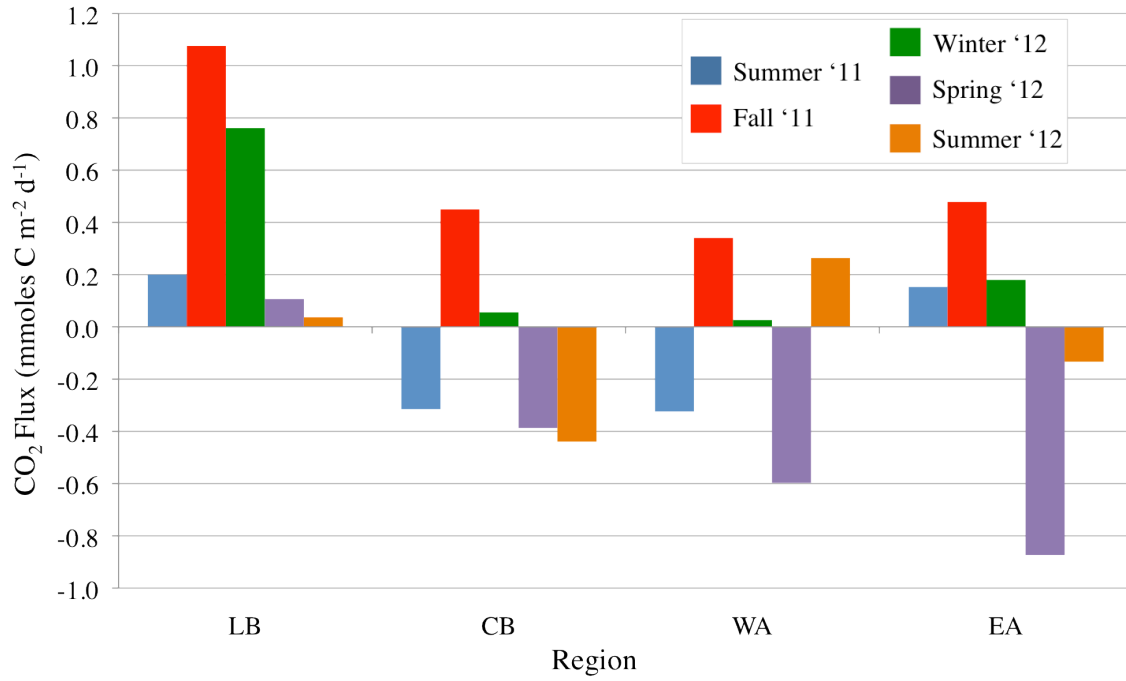
1



2

3 Fig. 6: Seasonal DIC vs. oxygen vs. depth - Scatter plots of DIC concentrations vs.
4 oxygen concentrations for each season between the summer of 2011 and the summer of
5 2012. Color bar represents depth in m. The red line depicts the C:O Redfield ratio of 106:
6 -170. Dotted circles highlight samples that deviate from Redfield.

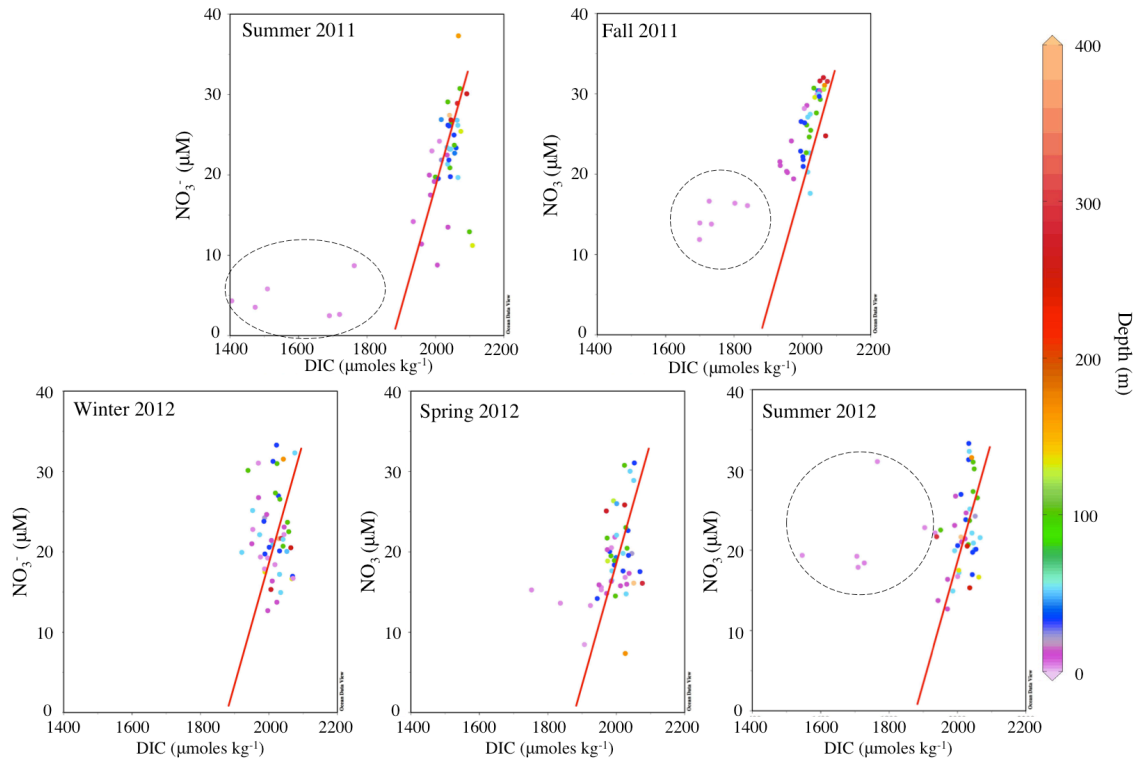
7



1

2 Fig. 7: Air-sea CO₂ flux – Seasonal air-sea CO₂ fluxes by region in mmol C m⁻² d⁻¹. Blue
 3 represents the summer of 2011, red = fall of 2011, green = winter of 2012, purple =
 4 spring of 2012, yellow = summer of 2012.

5



1

2 Fig. 8: Seasonal DIC vs. NO_3^- vs. depth - Scatter plots of DIC concentrations vs. NO_3^-
 3 concentrations for each season between the summer of 2011 and the summer of 2012.

4 Color bar represents depth in m. The red line depicts the C:N Redfield ratio of 106:16.

5 Dotted circles highlight samples that deviate from Redfield.

6